TALLINN UNIVERSITY OF TECHNOLOGY
School of Information Technologies

Fiorella Ines Soto Sanchez 221145IAFM

CONTRIBUTING TO THE DEVELOPMENT OF THE NEXT GENERATION NEUROPROSTHETIC DEVICE: DATA COLLECTION, PROCESSING, AND PROTOTYPE DEVELOPMENT

Master's Thesis

Supervisor: Alar Kussik
PhD

Co-supervisor: Jakob Rostovski
MSc

Tallinn 2022

TALLINNA TEHNIKAÜLIKOOL
Infotehnoloogia teaduskond

Fiorella Ines Soto Sanchez 221145IAFM

UUE PÕLVKONNA NEUROPROTEESI SEADME VÄLJA TÖÖTAMINE: ANDMETE KOGUMINE JA TÖÖTLEMINE, PROTOTÜÜBI ARENDUS

Magistritöö

Juhendaja: Alar Kussik
PhD

Kaasjuhendaja: Jakob Rostovski
MSc

Tallinn 2022

Author's Declaration of Originality

I hereby certify that I am the sole author of this thesis. All the used materials, references to the literature and the work of others have been referred to. This thesis has not been presented for examination anywhere else.

Author: Fiorella Ines Soto Sanchez

16.08.2022

Abstract

Loss of physical mobility and weakness of the lower limb muscles makes it complicated for individuals to participate in their day-to-day activities comfortably, even more, it poses a threat as the probability of falling increases. Current technological efforts in the field of assistive technology have developed powered wheelchairs, prosthetic limbs, functional electrical stimulation devices, and wearable exoskeletons to improve mobility. However, most studies involving neuroprostheses remain in the research phase and the commercially viable products follow an open-loop architecture that requires manual adjustments of devices during the operation. This thesis contributes to the development of a closed-loop and adaptive neuromuscular electrical stimulation system, which has been proposed by the Tallinn University of Technology and financed by the Estonian Research Council with the aim to support novel technologies that can adapt to the person's individual needs.

The thesis covers the data collection of human gait patterns using both an industry-standard inertial motion sensor and a new proposed and implemented measuring system, which consists of two BNO055 inertial measurement units (IMUs) and an ESP32 microcontroller. The gathered data was used to test the performance of abnormality detection algorithm developed within the PRG424 project of Estonian Research Council. Additionally, testing of textile-based electrical stimulation electrodes was conducted in the work.

Annotatsioon

Uue põlvkonna neuroproteesi seadme välja töötamine: andmete kogumine ja töötlemine, prototüübi arendus

Füüsilise liikuvuse kadumine ja alajäsemete lihaste nõrkus muudab inimeste jaoks keeruliseks igapäevastes tegevustes mugavalt osalemise, veelgi enam, see on ohtlik, kuna suureneb kukkumise tõenäosus. Praeguseks hetkeks on liikuvuse abitehnoloogiate valdkonnas välja töötanud elektrilised ratastoolid, proteesid, funktsionaalse elektrilise stimulatsiooni seadmed ja kantavad eksoskeletid. Enamik neuroproteesidega seotud arendusi on siiski veel uurimisfaasis ja kommertsiaalsed tooted põhinevad avatud (tagasisidestamata) arhitektuuril, mis nõuab seadmete manuaalset häälestamist kasutuse ajal. Käesolev lõputöö panustab suletud (tagasisidestatud) ja adaptiivse neuromuskulaarse elektrilise stimulatsiooni süsteemi arendamise, mille on välja pakkunud Tallinna Tehnikaülikool ja mida rahastab Eesti Teadusagentuur, eesmärgiga toetada uudsete tehnoloogiate arendusi, mis suudavad kohaneda inimese individuaalsete vajadustega.

Magistritöö käsitleb inimeste kõnnakuandmete kogumist, kasutades nii tunnustatud inertsiaalset mõõteseadet kui ka uudset kavandatud ja realiseeritud mõõtesüsteemi, mis koosneb kahest BNO055 inertsiaalandurist ja ESP32 mikrokontrollerist. Kogutud andmeid kasutati Eesti Teadusagentuuri projekti PRG424-projekti raames välja töötatud kõrvalekallete tuvastamise algoritmi testimiseks. Lisaks testiti töös tekstiilil põhinevaid elektrilise stimulatsiooni elektroode.

List of Abbreviations and Terms

AFO	Ankle Foot Orthosis
ML	Machine Learning
SVM	Support Vector Machine
NNs	Neural Networks
CNN	Convolutional Neural Network
MEMS	Micro-electromechanical Systems
FSR	Force Sensitive Resistor
FES	Functional Electrical Stimulation
IMU	Inertial Measuring Unit
TBI	Traumatic Brain Injury
MS	Multiple Sclerosis
TO	Toe-off
6-DOF	Six Degrees of Freedom
9-DOF	Nine degrees of Freedom

Table of Contents

List of Figures

List of Tables

1. Introduction

1.1 Problem statement

Physical disabilities derived from neurological or motor disorders are a global societal problem. It is estimated that 15% of the world's population, i.e., more than 1 billion people, live with some form of disability [1]. In the US 1 in 7 adults have a mobility disability, and the ratio increases to 2 in 5 in adults aged 65 and older. According to a study conducted by the National Center for Health Statistics, half the people presenting difficulties with physical functioning have a gait disability [2].

In the EU, an estimated 5 million citizens depend on wheelchairs due to gait dysfunction being the major cause of mobility disability [3]. Gait-related disabilities are mainly caused by central neurological conditions such as stroke, traumatic brain injury (TBI), Parkinson's and multiple sclerosis (MS), as well as musculoskeletal conditions associated with fall-related injuries, all of which have a higher incidence rate in the population over 65 years of age. Furthermore, a United Nations (UN) report stated that at present more than 1% of the global population is over the age of 80 years old and will rise to 4% in the year of 2050, and estimated number of people over 60 will outnumber those between 10 and 24 years old [4].

As the world's older population increases so do the costs of providing accessible healthcare. In 2010, a study conducted by the University of Copenhagen and the Department of Neurology showed that the European total annual cost was € 64 billion for stroke, € 33 billion for TBI, € 15 billion for MS and € 14 billion for Parkinson's patients [5]. Hence, the need to prioritize developing new assistive-technology devices and rehabilitation technology, which may in turn reduce the overall costs by providing enhanced, gradable, and highly reproducible systems. An example of an alternative way to treat and assist patients with gait impairments is functional electrical stimulation of the lower limb muscles (FES), which is used to stimulate dorsiflexion of the foot; this is an improved mechanism when compared to ankle-foot orthoses (AFO) since the walking speed and the average number of steps per day increase while diminishing the risk of falling. Nevertheless, some drawbacks of current FES models are their inability to recreate natural gait patterns and that they cannot adapt to different terrains robustly.

Thus, in a collaborative research project between the School of Information Technologies at Tallinn University of Technology, the East-Tallinn Central Hospital and the West-Tallinn Central Hospital, a new assistive technology device is being developed to only stimulate the weak muscles when necessary, based on real-time tracking of walking pattern deviations. The method consists of a closed-loop communication system to support highly responsive neuromuscular assistive stimulation and is specifically effective when it comes to the early detection of abnormal gait patterns on different terrains.

1.2 Goal and Objectives

This thesis's main goal is to develop and evaluate the performance of a new low-cost and non-intrusive mechanisms to collect human motion data in real-time. The present study is part of the PRG424 project that aims to realize and test a novel adaptive threshold shapelet-based algorithm to help people with gait disorders regain their mobility through a more accessible neuroprosthetic device that can adapt to their changing needs. This ongoing project is being developed by the Estonian Science Council in collaboration with Tallinn University of Technology. the East-Tallinn Central Hospital and the West-Tallinn Central Hospital.

To complete this task we must complete the following objectives:

- Developing and testing the hardware and software components pertaining to the dual-IMU data collection system and textile-based functional stimulation electrodes.
- Collecting volunteers' walking motion data using the developed prototype as well as an industry-standard wearable motion sensor (Shimmer3 IMUs) according to the clinical trial protocol approved by Estonian National Institute for Health Development, permission No.818.
- Processing and analyzing collected motion data recordings using a novel real-time abnormality detection algorithm developed within ETAG project PRG424, assessing algorithm's performance for different gait abnormalities.

1.3 Thesis structure

This thesis consists of five main sections, starting with the background section which will provide an overview of what are gait disorders and the current treatment options as well as the research trends in gait analysis and detection. This section will help the readers understand the underlying motivation to develop this prototype. The second section is about implementing the sensors using MicroPython, and it will also introduce a FES electrode design that will be used in the future to stimulate the user's compromised muscles or nerves accordingly.

The third section describes the experimental procedure and the data pre-processing steps. Then, the fourth section will focus on the testing and training the adaptive threshold shapelet-based algorithm and discuss the results obtained with both sensors. Finally, the fifth section will include the conclusion and future developments for this project.

2. Background

2.1 Gait disorders

Gait or walking involves repetitive cyclical activities of the lower extremities which result in bipedal locomotion. This mobility method involves multiple systems – nervous, peripheral sensory, musculoskeletal, and cardiopulmonary – which have evolved for the maintenance of stability to avoid posing a threat to the unsupported side during the stance phase of the gait cycle. When the stability of an individual is threatened, such as when walking on icy ground, people tend to widen their stance, prolong bipedal surface contact, avoid lifting their feet too high, slow down and shorten their steps. These strategies are employed both by young and older people to prevent fall injuries, however, with age muscle power diminishes as well as vision and proprioception, and because of those changes in mobility, the elderly suffer more frequently from gait disorders [6].

The underlying diseases that contribute to mobility disorders in adults are musculoskeletal gait disturbances, neurological gait disorders, and disorders associated with brain dysfunction. Musculoskeletal gait disorders are characterized by a limited range of motion, avoidance of weight-bearing, and limping. On the other hand, neuromuscular and myelopathic gait disorders can be detected on standard clinical neurological examination and tend to be caused by severe peripheral paresis. Gait disorders caused by brain injury in a sense belong to neurological gait disorders but present some disorders that are caused by spinal lesions [7].

2.2 Recent trends in assistive technology

The economic pressure of having an increasingly aging population is driving the global interest in developing assistive technology. Devices that enable self-sufficiency, independent living, and more efficient health monitoring. Unlike therapeutic technologies, assistive technologies encompass a broad range of devices that are designed to be operated by the user rather than by the clinician to promote functional activities in their home and community. They range from simple devices, such as crutches or canes, to more complex ones like robotic exoskeletons, or sensor-based person authentication software.

The rapid development and availability of enabling technologies, such as artificial intelligence (AI), augmented and virtual reality (AR/VR), robotics, Internet of Things (IoT), and new materials will play a key role in pushing the boundaries of assistive technology [8], as companies and research centers incorporate more of these technologies in their products. This paper will focus on describing the treatment options for foot drop syndrome, specifically those provided to people with intact peripheral nerves and preserved muscle tissues.

2.2.1 Foot drop

Foot drop (FD) is a common gait impairment derived from disorders, such as cerebrovascular accident (CVA) or stroke, spinal cord injuries (SCIs), multiple sclerosis (MS), cerebral palsy (CP), and brain injuries (BIs), which consist of paralysis or significant weakness of the ankle dorsiflexor muscles. It is characterized by an unusual high stepping motion to avoid dragging the foot during the swing phase of the gait cycle [9] . To analyze the human lower body locomotion mechanism, it is necessary to isolate the repetitive task during walking which is called the gait cycle. In Figure 1, the cycle is broken down into two main phases, the stance, and the swing phases. The stance phase consists of four sub-phases that start with the loading phase i.e., when the heel strikes the surface, and ends when the toe raises off the floor.

During the stance phase the weight of the body shifts completely on the foot and engages major muscle activity to complete the phase as subsequently, the weight will fall on the contra-lateral foot which propels the foot to the pre-swing phase. The swing phase starts when the toe lifts from the surface and reaches peak acceleration in the mid-swing sub-phase. Then the foot decelerates and reduces its velocity before restarting the cycle with the heel strike motion [10].

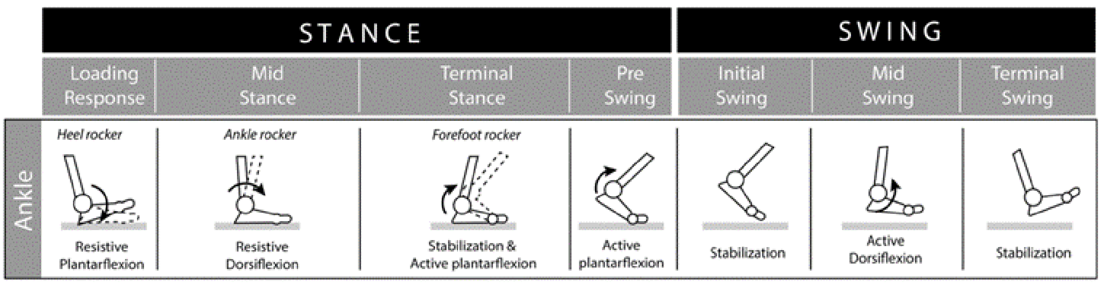

Figure 1. *Phases of the normal gait cycle. Source: [11].*

Brief description of the gait cycle [12] :

- Initial contact and loading phase (0-12%): the gait cycle starts with the initial contact of the heel against the surface involving the full extension of the knee and the contraction of the tibialis anterior gives place to the eccentric plantar flexion. The heel rotates to progress toward the loading response phase which stabilizes the body in preparation for the single limb support as the foot lies flat on the surface and absorbs the body impact [13].

- Mid stance (12-31%): The shank rotates forward generating the ankle rocker motion of the cycle. During this phase, the knee reaches maximum flexion, and the ankle becomes supinated and dorsiflexed [14].
- Terminal stance (31- 50%): This phase starts when the center of mass moves to the front of the supporting foot and the heel lifts away from the floor rolling onto the metatarsal heads, creating the forefoot rocking motion.
- Pre-swing (50-62%): The foot prepares to lift off the ground and the plantar flexion reaches 20° as the toes leave the floor.

Subsequently, the swing phase is divided into three stages [15]:

- Initial swing (62-75%): The knee and ankle start dorsiflexing releasing from the active plantar flexion, thus beginning the advancement of the limb forward.
- Mid swing (75-87%): The process of moving forward continues and the ankle becomes dorsiflexed by activating and contracting the tibialis anterior muscle.
- Terminal swing (87-100%): During this final stage of the gait cycle the shank advances for the last time and the foot returns to a neutral position and prepares positioning to start the next gait cycle.

Foot drop patients often do not land their heel first during the initial contact phase due to their inability to achieve adequate dorsiflexion and show uncontrolled plantarflexion during the swing phase leading to foot slap.

2.2.2 Foot drop treatment options

Current treatment options include physiotherapy, ankle-foot orthosis (AFO), surgery to fuse ankle and foot bones, tendon transfer surgery from lower leg muscles that have not been damaged and are still active, and functional electrical stimulation devices (FES). Generally, physiotherapy is prescribed when the cause of the ailment is suspected to be due to muscle weakness and the patient does not present nerve damage, but its application is limited by the patient's ability to exercise [16].

Ankle foot orthosis (AFO) is prescribed to alleviate various gait abnormalities and is often combined with physiotherapy to reduce fall risks; however, they are very bulky and painful when used for long periods of time. In addition, the AFO prevents the foot from dropping and forces it to stay at 90°, which does not help the patient regain muscle movement and forces them to walk in an unnatural manner [10]. Another treatment for foot drop is tendon transfer surgery, which has shown good results when the patient has left some ankle function intact. This treatment strengthens the area where the transfer has been made but may cause weaknesses in other areas. The surgery does not always correct foot drop and the patient might still need to use an AFO device afterwards. Neuromuscular electrical stimulation is recommended when the second motor neuron has not been compromised and the excitability in the peripheral nerves and muscle tissues are preserved, then neuromuscular electrical stimulation can be administered either to restore functional movement (functional electrical stimulation) or as a non-invasive analgesic treatment (transcutaneous electrical nerve stimulation) [17].

Functional electrical stimulation (FES) is particularly appealing as it is one treatment option besides physiotherapy that can help the patient recover their autonomy by treating the cause of the disorder and not the symptom. Nevertheless, FES devices are not suitable for patients that have widespread neural degeneration such as patients with mid-stage multiple sclerosis. Besides, the cost of a commercial FES can reach thousands of euros compared to € 100 for an AFO [18].

2.2.3 Commercial FES systems for foot drop correction

Functional electrical stimulation (FES) devices were introduced as a method to artificially evoke contraction in the paralyzed muscles and generate movements. It is widely used in gait restoration for neurologically impaired individuals. Since the 1960s when FES devices were first employed to treat stroke patients multiple FES-based neuroprostheses became commercially available, such as MyGait, ODSTOCK, etc. However, further improvements are required, such as building an adaptive system that modifies the stimulation settings based on the user's needs and environmental feedback [19].

Currently, commercial systems in the market range from externally worn portable surface stimulators, to partially implantable solutions. To the best of our knowledge, the commercial prototypes follow an open-loop system, hence most of the settings control are performed by the user with no real-time control of muscle stimulation.Furthermore, these devices operate based on gait-phase detection instead of stimulating according to gait deviations or abnormal behavior detection. Resulting in systems that cannot adapt to the persons' gait changes as they get fatigued, or lack mental focus. Below we compare the different FES-based commercial devices available in the market.

Open-loop systems: Commercial prototypes				
Device	Sensors	Modality	Muscles/nerves	Kit Price (€)[a]
MyGait	FSRs	Transcutaneous	Peroneal nerve	4420.00
ODSTOCK	FSRs	Transcutaneous	Unspecified	3940.00
Ness L300-Go	IMU	Transcutaneous	Tibialis anterior and peroneal nerve	6700.00
STIMuSTEP	FSRs	Implanted	Peroneal nerve	7640.00
ActiGait	FSRs	Implanted	Peroneal nerve, tibial and peroneal muscles	16,740.00
Fesia Walk	IMUs	Transcutaneous	Tibialis anterior and peroneal nerve	-
Medical XFT-2001D	MEMS	Transcutaneous	Peroneal nerve	2930.00
WalkAide	Tilt sensor	Transcutaneous	Tibialis anterior and peroneal nerve	4115.00

[a]Sources used to find the cost of the devices , [20], [21], [22], [23]

2.2.4 Gait event detection

Gait event detection (GED) is a crucial component when designing foot drop neuroprostheses, such as an electrical functional stimulation device, since they operate based on a gait-phase detection mechanism, i.e., they identify the initial contact and loading response of the foot using either a foot switch or an inertial sensor.

The first FES prototype proposed by Liberson used a heel switch that triggered the tibialis anterior muscle and required careful handling of the stimulation settings which had to be done manually [24]. Meng et al, used the same principle but tried a multichannel approach to stimulate more muscles, which resulted in a better representation of normal gait patterns [25]. However, the timing of the stimulation was still rigid, and the person had to manually adjust the settings.

Numerous studies continued to focus on detecting the stance and swing phases using diverse types of sensors ([26], [27], [28]). For instance, force-sensitive resistors (FSRs) were placed under the heel and forefoot of both feet to detect the heel strike, heel-off, and toe-off events in real-time. However, the results showed problems when detecting the swing sub-phases and the performance was subjected to the location of the FSR sensors. On the other hand, inertial sensors (accelerometers, gyroscopes, and magnetometers) do not depend on the surface or footwear used and can be used to create closed-loop control algorithms calculating the kinematic parameter, but this is still under research.

In 2013, Chen et al., developed a real-time transcutaneous self-adaptive system that employed FSR sensors located under the heel to estimate the step frequency and predict the swing phase from previous steps. The system detects the angular velocity and the step frequency so that the stimulation applied to the tibialis anterior muscles adapts based on the feedback of a long short-term memory (LSTM) neural network. The study had positive outcomes but struggled when the walking speed increased because of the difficulty to predict the step frequency [29].

Another study conducted at the Technical University of Berlin proposed a transcutaneous stimulation system called APeroStim that consisted of a small 6-DOF IMU sensor attached to the foot. Various data representing different gait events (swing phase, heel contact, and TO) were collected to test a closed-loop threshold-based system that adapts to the walking speed of stroke patients [30]. Similarly, Valtin et al., developed a transcutaneous feedback-controlled foot drop neuroprostheses that used a wireless inertial sensor located on the foot to detect gait phases and foot orientation measurements. The algorithm used was the same one that had been developed during the AperoStim project that used gait phase o trigger muscle stimulation at the TO event as well as enabling the control of the ankle's dorsiflexion and eversion during the swing phase [31]. The study showed the possibility of having a standalone FES system that included external wireless sensors and sophisticated data processing, however, it remains under investigation and has not been commercialized. Further understand of long-term effects of such devices needs to be conducted to determine their clinical potential.

2.3 Review on trends for gait analysis using ML techniques

Recently gait data processing and learning algorithms have been shifting from statistical methods toward Machine learning because of their high accuracy in processing gait parameters based on the field of application. They offer the possibility of building automatic systems able to distinguish healthy subjects from patients affected by neurodegenerative diseases or to detect the different levels of the disease from early to severe stage. The data collection is performed by employing wearable or non-wearable solutions to extract or select features to construct models and use them to predict the likelihood of the new data falling into a determined target class.

To the best of our knowledge, current research focuses on developing machine learning algorithms that trigger muscle stimulation based on gait event detection instead of tracking real-time anomalous gait behavior. The gait phases described in section 2.2.1 follow a unique sequence of movements that facilitate the design of various applications in different fields such as healthcare, security, sports, and fitness. Since the end goal of the PRG424 project is to develop a wearable device that can track human- motion we will be only be reviewing machine learning algorithms based on wearable sensors. Figure 2 provides an overview of the wearable sensors used in gait analysis.

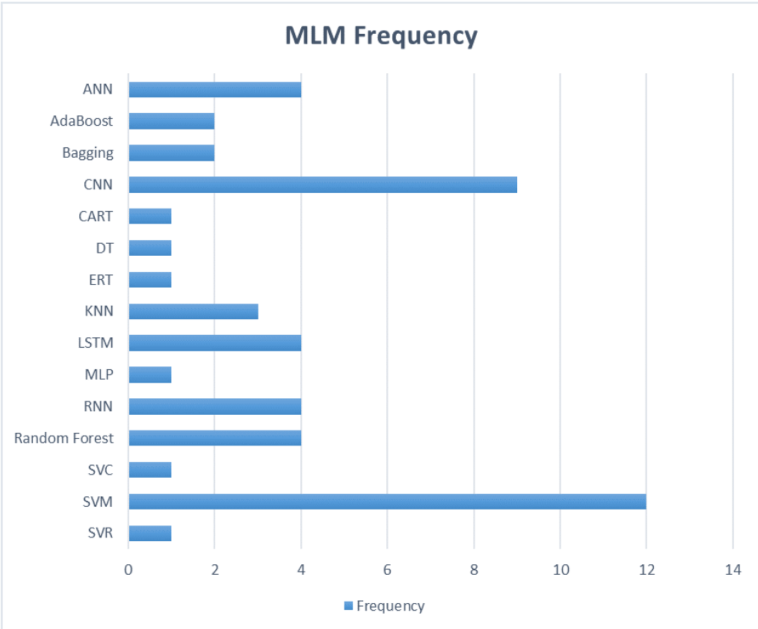

Figure 2. *Frequency of Machine Learning methods found in selected papers reviewed to analyse the recent trends in gait analysis. Source: [15]*

A paper on the latest Machine Learning trends in gait analysis showed that the most frequently used algorithms were SVM and CNN [15]. The selection of SVM is primarily driven by its ability to generate improved predictive models faster than other deep learning technologies and that, unlike NNs, SVMs can perform well when the dimension of the input data is high, and the size of the data observations is small. On the contrary, CNN-based gait analysis systems have complex structures and are computationally expensive, but they are typically used for gait recognition due to their accurate results as well as their ability to learn automatically useful features of large input data [32].

Chelli et al, proposed a machine learning framework for fall detection and human activity recognition (HAR) using the mean value of a triaxial accelerometer and achieved a fall detection accuracy of 96% and precision of 100%. Furthermore, the paper assessed the performance of four different classification algorithms, artificial neural networks (ANN), K-nearest neighbors (KNN), quadratic support vector machine (QSVM), and ensemble bagged tree (EBT). When they used both the acceleration and angular velocity data the results showed that KNN had the lowest accuracy result of 85.8%, followed by ANN with an accuracy of 91.8%, then the two best-performing algorithms were QSVM and EBT achieving an overall accuracy of 96.1% and 97.7%, respectively [33]. Hakim et al, also reported good accuracy results using an SVM model in an earlier study where he employed a smartphone (Sony C6002 Xperia Z) that featured an embedded 6-DOF IMU. The study also evaluated the performance of four machine learning algorithms (SVM, Decision Trees, Nearest Neighbor Classifiers, and Discriminant Analysis) and the results revealed that the SVM model achieved accuracy values above 90% for all the four types of activities simulated [34].

2.3.1 Summary

This section focused on explaining the necessary background information to understand the project's underlying motivation in developing an affordable alternative to treat and aid people with foot drop syndrome to regain their independence. The conventional approach has been the application of AFOs, but because it does not provide enough assistance other alternative solutions such as applying functional electrical stimulation (FES) have gained popularity due to their orthotic and therapeutic effects. Moreover, there have been several studies integrating machine learning in the development of more robust closed-loop FES systems. These studies, however, are still in the research phase and are not commercially available. Furthermore, we saw that these studies focused on gait phase and event detection using IMU sensors which showed some limitations when required to function in real-time scenarios as they depend largely on how efficiently they can detect gait sub-phases.

3. Hardware development and testing

Numerous papers have proposed different approaches to designing FES systems to perform as neuroprostheses or aid patients in their recovery, both commercial and research-stage FES devices were mentioned in Chapter 2. The research shows that IMU-based gait detection methods have higher accuracy when data is collected from the region of the metatarsophalangeal joints [35] as well as collecting data from the knee and hip joints when dealing with abnormal deviations from the hip and knee, as is the case with hemiplegic gait. It is known that hemiplegic walking shows decreased motion in the hip and knee coordination [36]. Therefore, as part of the PRG424 guideline, we were required to build a measuring system that implemented at least two IMU sensors and was compatible with the adaptive threshold algorithm written in Python.

The purpose of this chapter is to showcase the proposed gait deviation measuring system since the Shimmer3 sensors do not support the use of two IMU sensors. Firstly, this section introduces the elements used to build the hardware component of the prototype which consists of two 9-DOF sensors, and the ESP32 WeMos Lolin32 Lite, a low-cost microcontroller with an extensive set of peripherals including Wi-Fi and Bluetooth wireless capabilities. Secondly, we discuss the process of coding and configuring the sensors, as well as the problems we encountered. Finally, we discuss if the proposed FES electrode prototype design is suitable to be applied as a smart wearable for muscle stimulation.

3.1 Implementing the prototype sensors (BNO055)

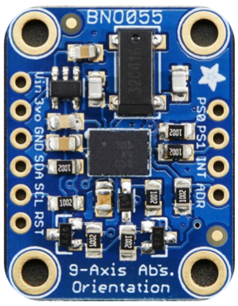

Figure 3. *Adafruit's BNO055 Sensor Board*

The developed system for gait analysis is composed of two IMU BNO055 sensors, shown in Figure 3. The sensor consists of a triaxial accelerometer and triaxial gyroscope, which will be connected to a microcontroller (ESP32 WeMos Lite 32). During walking, linear acceleration, and angular velocity signals will be measured by the BNO055 sensor.The sensors have been placed on top of the foot-bridge (metatarsal region) and below the knee.

The sensors below the knee level and on the footbridge had an acceleration range of ±4g with a Sensitivity Scale Factor of 500 (LSB/g) and a gyroscope range of ±2000 deg/s with a Sensitivity Scale Factor of 16.4 (LSB)/deg/s. Furthermore, the digital signals generated by the BNO055 sensors through an I2C interface are collected by the ESP32. The microcontroller possesses a Bluetooth module for wireless communication. The output signals of the accelerometer and gyroscopes aim to be sampled at 100 Hz which is sent simultaneously to an iOS smartphone app 'LightBlue'. The schematic diagram of the designed system is shown in Figure 4.

The selection of this sensor was made mainly because it has been used in prior research studies made by the Department of Electronics at Tallinn University of Technology. Furthermore, the sensors conform to the requirements of the project as they are affordable, easy to implement, and have a low power consumption. Similarly, they have been used for time-series data applications, human activity recognition problems, tracking and navigation problems, etc [37], [38]. .

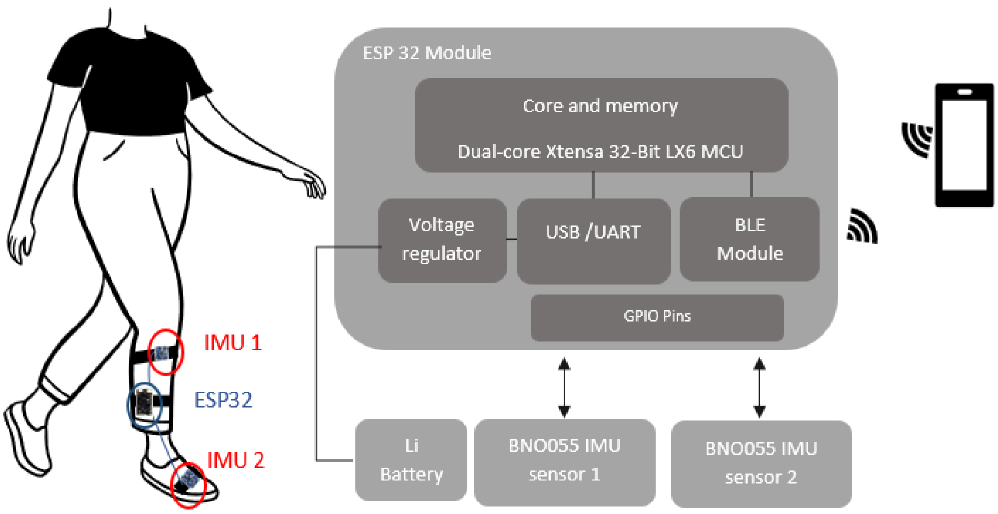

Figure 4. *Block diagram of the measuring system prototype. This figure shows the location of the sensors on the body. It also depicts the components of the prototype and the communication protocol used to send the data in real-time.*

At first, the BNO055 sensor was connected to the ESP32 development board. The sensor has a Vin pin (3,3V output) which was connected directly to the ESP32 3,3 V pin. The ground (GND) pin was connected to the GND in the ESP32 board, SDA (I2C clock pin)

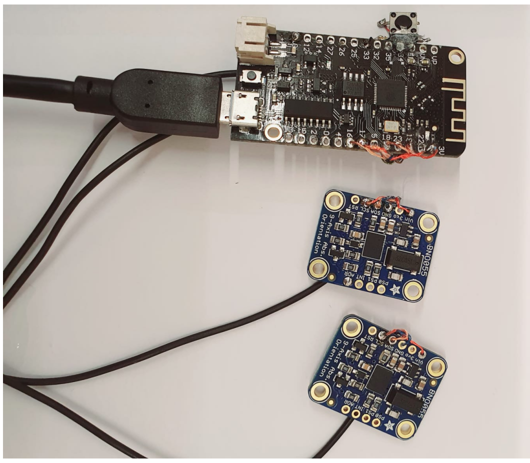

Figure 5. *Implemented hardware prototype consisting of WeMos ESP32 controller and two BNO055 inertial sensor boards.*

to ESP32's pin 18, and SCL (I2C data pin) to pin 19. The second sensor was initialized in the same microcontroller. Its wiring was the same as the first sensor; except that the ADR pin was also connected. ADR changes the default I2C address to avoid a crash with the first sensor.

3.2 Implementing the sensors software

MicroPython was used to program the measuring system so it would be compatible with the adaptive threshold shapelet-based algorithm developed earlier by a member of the PRG424 project. To obtain the data collected by the BNO055 sensors, we have used the Adafruit library [39] as well as the MicroPython low-level Bluetooth module [40]. Initially, we attempted to use the multi-threading approach to separate the tasks and avoid delay and memory errors. As described in Algorithm 1, the multi-threading approach consisted of initializing two threads using the module _thread, to perform the reading/sensing of the acceleration and angular velocity every 10ms and then writing/sending the data through the serial Bluetooth port. Additionally, we employed simple mutexes to synchronize the tasks, so that the writing sequence would only start after the sensing occurred. Thus, thread 1 would only run once the mutex write_the_data switched to True, which was scheduled using the Timer module. The mode chosen was periodic and the callback function triggers the while loop in thread 2 every 10ms.

The results of the first algorithm were not satisfactory because of inconsistent data readings as well as in some cases duplicate readings. Hence, we opted to simplify the model and use one thread instead of two as seen in the description of Algorithm 2. This approach reduces the use of mutexes and removes the use of queues. Regardless, of simplifying the code the readings were still not able to reach a rate of 10ms, instead, we obtained consistent readings at a rate of 20ms most of the time, and sometimes the data would log in 30ms or less. Figure 6 shows the results obtained with the multi-threading approach, the y-axis shows the fluctuation of the sampling time indicating that the sensors are not logging data consistently and thus not complying with our requirement of having reliable measurement readings at a sampling rate of 100 Hz. Figure 7 shows the improved results when implementing the single threading algorithm, we still see some fluctuations but these are variances of approximately 10ms and do not happen very often. Furthermore, we can apply re-sampling and linear interpolation techniques to fix the varying sampling rate frequency.

Algorithm 1 Multi-threading

```
Thread 1
while write_the_data = True do
    Call function writer.send()
end while
Set flag variable write_the_data = False
Thread 2
while read_from_sensor = True do
    Start timer t_sense = ticks_ms()
    Call function to take readings from sensors
    Add the timestamps(t_sense) to the readings
    Append and store output and save in the global variable data
end while
Set flag variable read_from_sensors = False
set flag variable write_the_data = True
```

Algorithm 2 Single thread

```
Initializing th_sense_data_running = True
Initializing read_from_sensor = False
Thread 1
while th_sense_data_running = True do
    Start timer t_sense = ticks_ms()
    try: Call function to take readings from sensors
    Add the timestamps(t_sense) to the readings
    Append and store output and save in the global variable data
    try: Call function writer.send()
    Set flag variable read_from_sensor = False
end while
Handling function: switches the read_from_sensor mutex to True
Callback argument: we will set the timer to fire periodically each 10 ms, calling our
previously declared handling function.
```

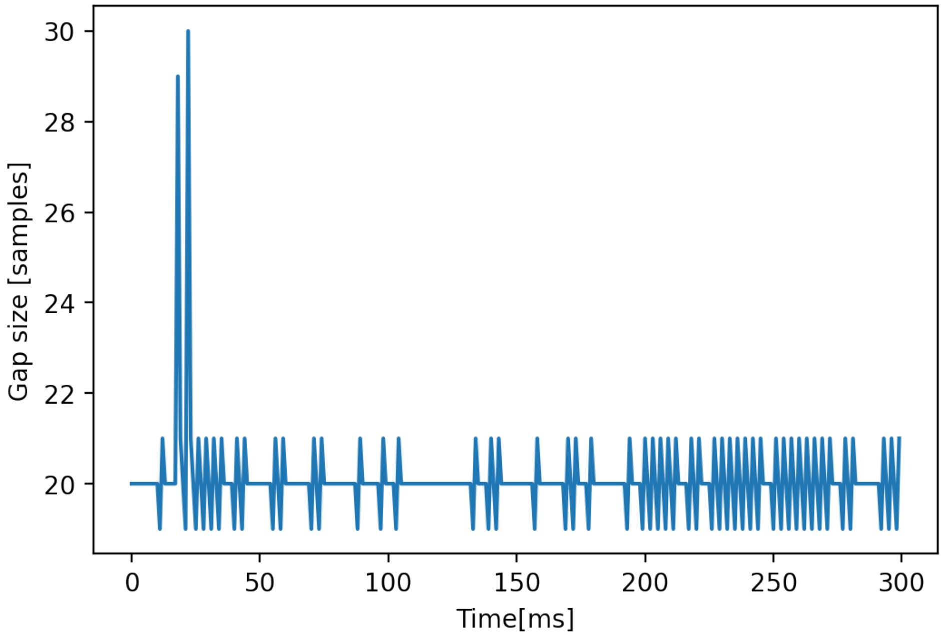

Figure 6. *Gap size using the multi-threading approach.*

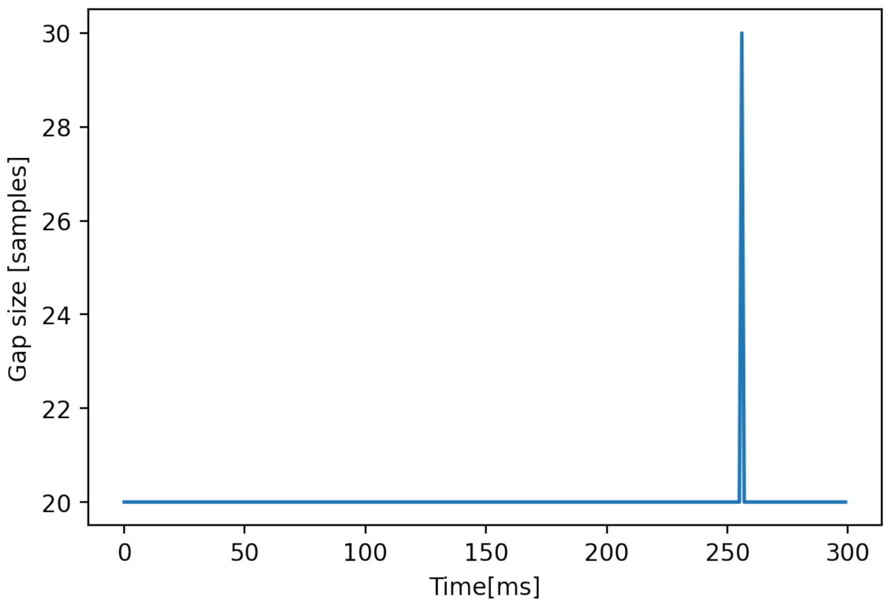

Figure 7. *Gap size using the single threading approach, we get more consistent readings taken at periodic intervals of 20ms.*

3.3 Implemented software tools

The prototype deployed the latest MicroPython firmware .bin, which at the time was the esp32/GENERIC firmware esp32-20220117-v1.18.bin as well as installing Python 3.10 on our windows PC. Below we describe the required tools to develop the software component of the project.

1. Visual Studio Code

For this thesis we have chosen Visual Studio Code (VS code) which is a source code editor that supports many programming languages (licensed or open code) and possesses many handy features listed below. furthermore, other members involved in the PRG424 project were using this IDE, so in order to avoid inconsistencies in the configuration the same development environment was used.

- **Cross-platform**: VS code can be installed across all three main operating systems (Windows, Linux and Mac OS).
- **Intellisense**: Its a language service that enable the ability to predict the instruction to be written based on language semantics and analysis of the source code. Which help us avoid making typing errors and speed up the writing process.
- **Debugger**: VS code allows you to make changes and and debug the program on the go step by step without having to print and recompiling.

2. Python 3

The ESP32 microcontroller does not come with a MicroPython port incorporated, so we need to load the interpreter first. To install MicroPython on the ESP32 we first installed the latest version of Python (Python 3.10). Python is required because of the python-based tool used to communicate with the ROM bootloader in the ESP32 chip, i.e., **esptool.py**. Once esptool.py has been installed then we proceed to flash MicroPython into the ESP32.

3. Required libraries

C or C++ are the most commonly used languages to program microcontrollers due to their runtime efficiency and in the case of C++ it provides access to many standard libraries. However, we opted for a programming language that would be compatible with the adaptive threshold shapelet-based algorithm which has been developed with Python. We used the following libraries to design the code.

- **micropython-bno055**: Library for the Adafruit BNO055 sensor that is designed to run on any hardware that supports the *machine* module on the I2C interface.
- **Machine**: This module contains specific functions related to the hardware on a particular board. Used amply to control the hardware block on the ESP32 board, we imported the Freq (get the CPU frequency), Timer and Pin power functions.
- **Time**: provides access to time delays,intervals, etc., from which we used the *time_sleep, time_ticks, Periodic scheduler* and the interrupt handlers. In our code we are setting our main loop to 150000 milliseconds.
- **_thread**: This library offers multithreading support. We have implemented a single thread simplifying the code by removing the use of locks and mutexes, and combining the threaded functions in one.
- **ubluetooth**: Gives bluetooth access to the Bluetooth controller board. Micropython only supports low-level Bluetooth connection in roles such as central, peripheral and broadcaster. We followed the example posted by [41].

3.3.1 Summary of dual-IMU wearable sensor development

In this section the design and implementation of the hardware component of the neuroprosthesis was presented, which consisted of two BNO055 sensors and the ESP32 microcontroller. During the software configuration we described the implementation of a multi-threading scheduling mechanism and a single thread algorithm using the timer interrupt module to trigger the readings every 10ms. The performance of the prototype was compromised due to MicroPython's code interpretation not being fast enough to sample data at a high rate or due to issues with the software's kernel scheduler. As a final remark it is recommended in the future to employ a different microcontroller platform, perhaps opting for a compiled programming language so that the system runs faster whilst being more stable.

3.4 FES electrode prototype testing

The goal of the design was to develop an unobtrusive system that stimulates the lower leg muscles. The device would have embedded electrodes placed on: the tibialis anterior, nervus peroneus, and the fibularis longus.

We opted for socks as the medium to implement our electrical stimulation system for daily use as people wear them to perform various types of activities, and therefore resistance to wearing socks is low. Moreover, the socks are custom-made so that the electrodes are placed correctly based on their needs, and have a tight fit to prevent them

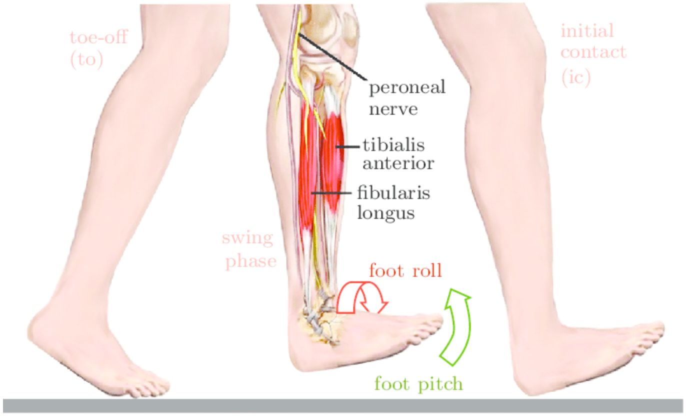

Figure 8. *Muscles and nerves involved in the dorsiflexion of the foot and ankle. Source: [42].*

from sliding down. This aims to make them effective for stimulating the right muscles and allowing the electrodes to remain in contact with the skin without significant displacement.

3.4.1 Electrodes Position Design

The position and number of electrodes were determined by physiotherapist Mr. Heigo Maamagi, who is part of the project PRG424. As shown in Figure 9, the electrodes were placed on the target muscles of the lower left leg. Position **(A)** was located on the tendon of the tibialis anterior, **(B)** on the nervus peroneus, and **(C)** on the fibularis longus.

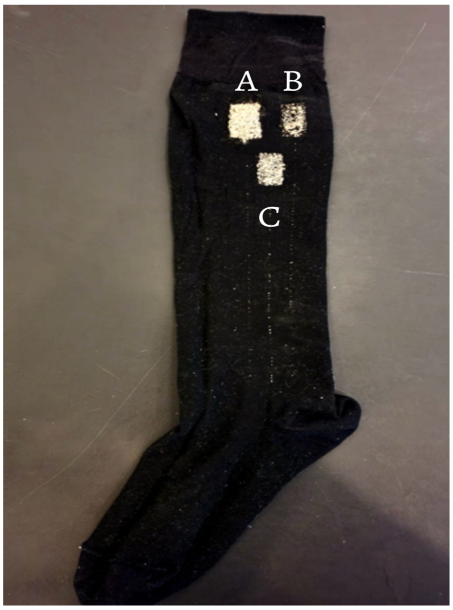

(a)

(b)

Figure 9. *(a)Sock with silver thread electrodes and leads (b) Physiotherapist trying the sock on to check the correct placement of the electrodes.*

3.4.2 Selected materials

To implement the prototype the electrodes should be made of fabric. In this study, we used two different materials, one used conductive fabric and the other silver thread. Figure 10 shows both designs of the conductive fabric electrodes. There are three snaps per sock and are located on the outer layer of the sock. To test the conductivity of the socks and verify that the device delivers pulses of electrical energy we used a transcutaneous electrical nerve stimulation (TENS) device, the Sanitas digital electronic muscle stimulation device —SEM 44.

Figure 10. *left: Conductive fabric electrodes with wire covered insulating coat, right: Silver thread electrodes.*

3.4.3 Feedback and remarks of the FES electrode prototype

The problems identified by the physiotherapist were related to comfort and the lateral displacement of the electrodes. Even though, the socks were custom-made the position of the electrodes were slightly off, specially the electrode placed on the digitorum longus muscle in charge of the extension of the lateral four toes, and dorsiflexion of the foot. As seen in Figure 11, electrode A should have been placed closer to the tibia and electrode C on the lateral side of the leg.

Using the Sanitas 43 EMS/TENS device we tested the conductivity and performance of the smart socks. The set amplitude increased gradually starting at 15mA, which was the default setting obtained by the manufacturer, and the final amplitude was 30mA. That intensity was uncomfortable when using the dry electrodes, it was described as *"... the pulses feel like pins and needles burning the skin".*

The most uncomfortable electrode design was the one with conductive fabric and the insulated wires, even when it was set to a low amplitude intensity where the muscle stimulation was not visible the subject asked us to stop because the pain was intolerable.

(a)

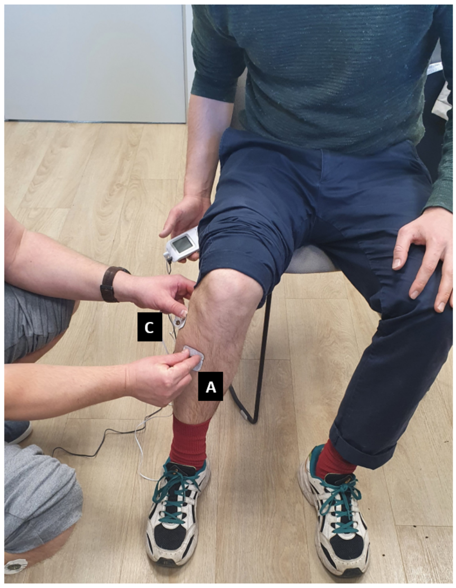

(b)

Figure 11. *(a)Smart sock prototype on the left leg (b) Dry electrodes placed on the Anterior Tibialis and over the fibula head near the common peroneal nerve.*

Hence, we continued the experiment with the silver thread electrode design and found that at 30mA amplitude, 310 microseconds pulse width, and 60 Hz frequency we could stimulate the ankle dorsiflexion and if we moistened the electrodes the pulses were more stable and comfortable for extended usage. Nevertheless, the configuration of the pulse frequency and width as well as the intensity will vary based on the user's needs and preferences.

3.4.4 Summary of textile FES electrodes testing

The FES electrode prototype was evaluated to determine its applicability for muscle stimulation to aid patients with foot drop syndrome. The evaluation was carried out by a licensed physiotherapist and one able-bodied subject using the Sanitas electrical muscle stimulation device. The experimental results demonstrated that the silver threaded yarn prototype performed better in terms of stimulation delivery when the electrodes were moistened. Nevertheless, when the electrodes dried within a couple of minutes the fabric electrodes caused inconsistent and unpleasant stimulation.

Further work on the design is needed as the tightness and impracticality of electrode displacement requires future improvement. The concept offers a promising alternative but more testing involving patients with gait impairments is required to identify their needs as this evaluation was limited to a single able-bodied participant.

4. Data collection and annotation

This section describes the hardware and software settings employed to collect the pertaining data. Also, shows the experimental protocol for both experiments and the sensor implementation on the test subjects. The experimental protocol described in this section complies with the clinical trial guidelines approved by Tagasisidestatav andmevahetussüsteem kõrge reaktiivsusega abistava neuromuskulaarse stimulatsiooni võimaldamiseks, Tervise Arengu Instituudi inimuuringute eetikakomitee, Otsus nr 818.

4.1 Data collection using Shimmer3 IMU sensor

The Shimmer3 sensor is an inertial measurement unit electronic device that consists of a 3-axis accelerometer (which measures linear acceleration), a 3-axis gyroscope (which measures the angular velocity, and a 3-axis magnetometer (measuring magnetic field), all with a respectable range [43]. This sensor was selected based on the project's use case since it is pervasive in the healthcare field and it offers the Consensys software that alongside the sensor base provides added features such as sensor configurations, logging processing data, and data management.

The sensor configuration used for this study replicates the one made by [44]. The author first tries to collect data with the default settings and finds excessive gaps when logging data in real-time, then he adjusts the wide-range accelerometer and the gyroscope values. The final configuration reduces the gaps incidence to 4 found in 14000 samples.

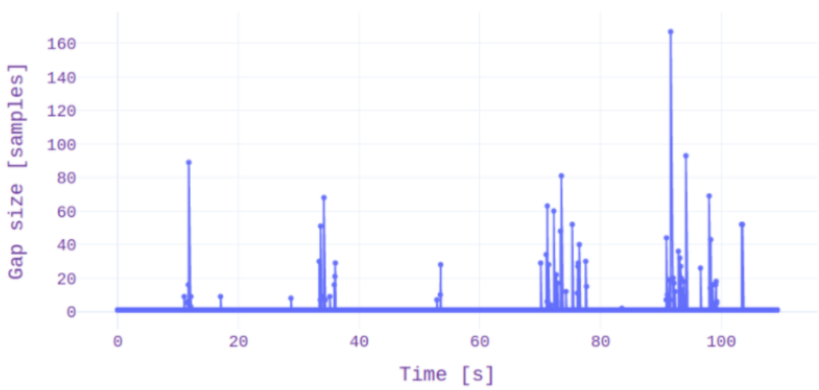

Figure 12. *Configuration following the default settings.Source: [44].*

The acceleration and angular velocity are measured at 256 Hz. Each unit consisted of a tri-axial accelerometer (range: 8 g) and a tri-axial gyroscope (range: 1000 dps). The

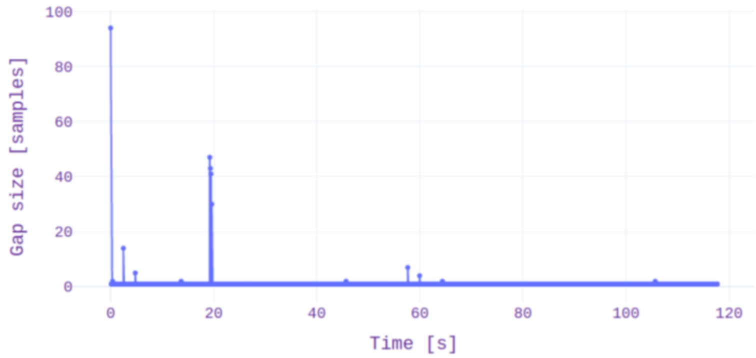

Figure 13. *Final improved configuration with less data gaps.Source: [44].*

sensor units were mounted below the knee level and the other was mounted on top of the participant's shoe. The measurements from the right leg were included in the experiments. Figure 14 shows the sensor placement on the shoe and the axes definition.

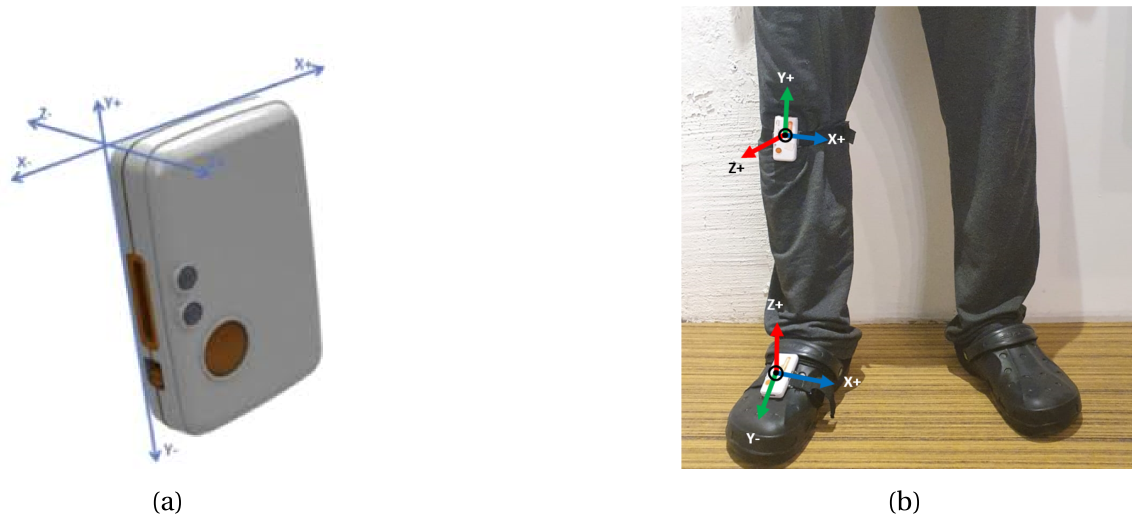

Figure 14. *(a) A Shimmer3 device and its reference coordinate system. (b) The alignment between sensor's axes and body reference system.*

4.1.1 Experimental protocol

A group of twenty volunteers participated in the experiment. The subjects had no musculoskeletal or neurological dysfunctions and provided written informed consent prior to participating in the experiments. The general information about the subjects is given in the following table. Participants walked freely at a comfortable, self-chosen speed in an obstacle-free and flat environment for 6 × 10 m. After 10 steps of normal walking, participants were instructed to simulate a gait disorder with the leg that had the sensors mounted.

Table 1. *Subjects' Information Used In This Study (Mean ± Standard Deviation)*

No. of subjects	Age (years)	Height (cm)	Mass (Kg)
14 (Male)	32.7±11.1	178.2±5.5	77.7±15.1
6 (Female)	26.9±5.5	169.4±6.2	64±8.9

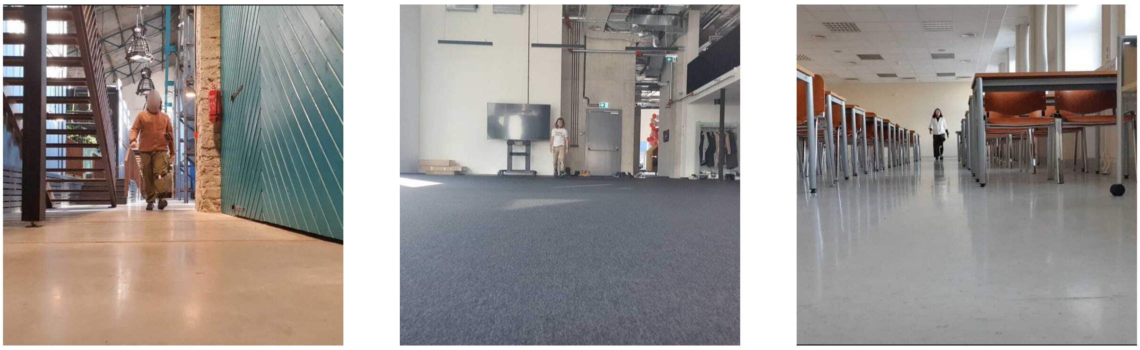

Figure 15. *Multiple sites where the experiment was conducted: Hektor Container hotel (left), Mindvalley Office (middle), and TalTech Classroom (right).*

Gait simulation

The participants were instructed to walk in a straight line and turn at the end of the corridor, this process was repeated six times for each gait disorder simulated, i.e., 60 meters which included at least six abnormal gait patterns. The goal was to collect very distinct gait patterns so that the normal and abnormal strides could be easily categorized and segmented when annotating the data. Due to weak haptic feedback of the shimmer3 sensors sometimes the data was not recorded, hence we performed when possible two trials per gait abnormality simulated. The frequency of normal and abnormal steps varied depending on the location of the experiment as well as the gait disorder simulated. The gait disorder simulation was divided into two groups, the first one consisted of the ataxic, diplegic, and parkinsonian gait disorders, and the second group entailed the steppage, antalgic, and hemiplegic gaits. Table 2 shows the different configurations for the simulation. Since the equipment used in the experiment was portable we could conduct the experiment in different settings as seen in Figure 15.

Table 2. *Simulation Configurations*

Location (Walking distance)	**Group 1**	**Group 2**
Hektor (12 meters)	9 normal + 3 abnormal	10 normal + 1 abnormal
Taltech classroom (10 meters)	7 normal + 3 abnormal	8 normal + 1 abnormal
Mindvalley office (10 meters)	7 normal + 3 abnormal	8 normal + 1 abnormal

4.2 Data collection using prototype sensor

4.2.1 Experiment

The experiment protocol followed the same guidelines as the one with the shimmer3 sensors, but due to time constraints the experiment was conducted with only three participants. The anthropometric data of the participants are shown in Table 3. To evaluate the performance and feasibility of gait detection of the designed prototype it will be used together with the Shimmer3 sensors so that they are exposed to the same conditions. Two synchronized IMUs acquired data at 50Hz and the data was transferred via Bluetooth to a personal smartphone for data logging. In this study, the LightBlue smartphone app was used on iOS to connect to the ESP32 GATT server.

Table 3. *Anthropometric data of the partcipants (Mean ± Standard Deviation)*

No. of subjects	Age (years)	Height (cm)	Mass (Kg)
3 (Female)	33±20.5	161.9±7.2	61.2±4.7

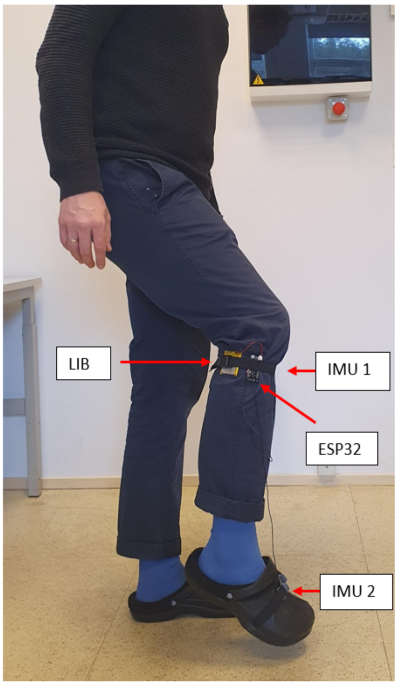

Figure 16. *Model picture of the instrumentation with the BNO055 sensors (S1,S2).*

4.3 Data annotations

Data annotation involves the process of labeling and identifying data in various formats like text, images, and videos [45]. In our case, we will be annotating the data collected and exported with the Shimmer3 sensor and Consensys software. Our region of interest lies in identifying the abnormal gait patterns within the WAV files generated using a python script written by PRG424 member,which helps us easily distinguish the steps and turns. Additionally, the script creates an automatic text file that assigns an "OK" label for each right footstep.

To start the data annotation process, we first installed VirtualBox to then install Linux, but because there were some issues with transferring data from our Windows PC to the Linux environment we later then switched to VMWare, refer to table 4 for further system specifications. Subsequently, we downloaded Audacity, a multi-track audio editor, and set up the Anaconda navigator to launch the Spyder IDE for compiling the python script.

The python script was developed to annotate the sensor data automatically, it allows you to adjust the threshold values and the default label boundaries [44]. If the start and finish points are correctly labeled automatically or by adjusting the threshold values, then the output will be a WAV file (audio file) and text file. Otherwise, we will need to ignore the label generating function and instead manually create a text file. Following the audio and text file generation, we proceed to review the data using Audacity.

As seen in Figure 17, the text files only show “ok” signals as the default value. Thus, we need to adjust the beginning and the end of all step cycles and label the normal and abnormal gait patterns based on step count, recordings of the participants, and visual characteristics.

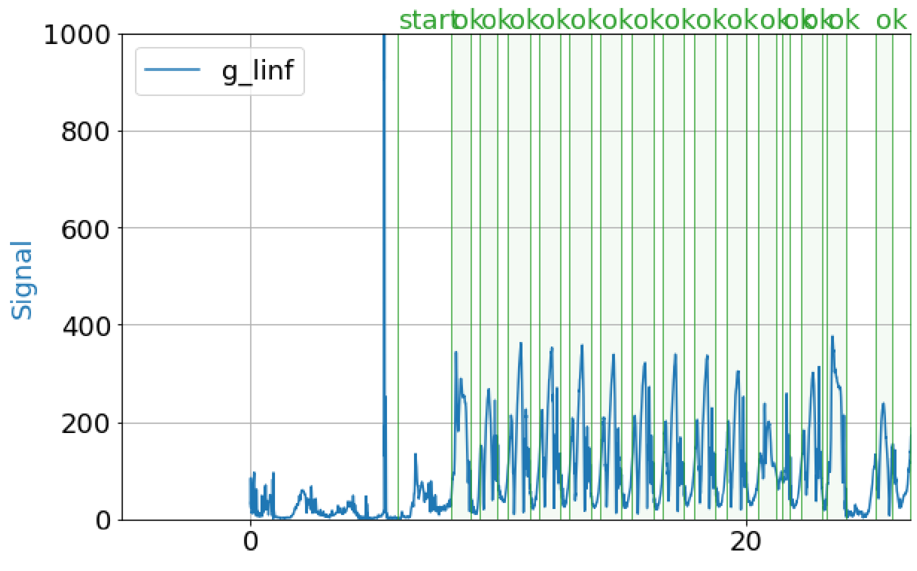

Figure 17. *Automatically generated audio file with text annotations.*

Table 4. *System specifications*

Processor	Intel(R) Core(TM) i7-10750H CPU @ 2.60GHz 2.59 GHz.
Installed RAM	16.0 GB (15.8 GB usable).
System type	64-bit operating system, x64-based processor.
Windows Edition	Windows 11 Home.
System	Linux Mint 20.3 Cinammon V.5.2.7,base:Ubuntu 20.04 focal.
Linux Kernel	5.4.0—107—generic x86_64 bits: 64 compiler: gcc v: 9.4.0 .

4.3.1 Summary of gait data collection

This section entails the most critical and time-consuming tasks of the paper. Recruiting participants, collecting the data, and processing it. Overall, there were 192 files of data per sensor from 20 participants using the Shimmer3 inertial sensors and 81 files generated both by the Shimmer3 and the prototype sensors from 3 different participants during the second phase of the experiment. The participants performed simulations of six different gait disorders, but not all files were used due to time constraints and the data having some errors (data is too short, data labeling – data concatenation errors, missing data points, etc.). Moving forward more experiments need to be conducted with the prototype sensors as we were limited to only testing with three able-bodied participants. It should be noted that this experiment did not consider factors such as fatigue in the experiments, as participants walked for approximately 2 minutes per gait disorder simulation.

5. Collected motion data classification using a ML algorithm

In this section the adaptive threshold shapelet-based algorithm developed by a member of the PRG424 project is presented. The training and testing of the algorithm was performed using 13 participants data files with 144 recordings from the sensor placed on top of the footbridge. The algorithm provided objective base master metrics (TPR, FPR, accuracy, and F1 score) of the overall performance per data set, taking into consideration each gait abnormality. A complete view of the collected data cannot be presented here due to time limitations to process all the data and for brevity.

5.1 Brief description of the novel threshold based algorithm

In section 2 different ML trends in the field of gait analysis were discussed showing that the main focus resides on developing classification methodologies that perform feature extraction and feature selection to construct models, so that they can be used later to predict the likelihood of the new data falling into a determined target class [46]. However, to the best of our knowledge, there are no machine learning classification algorithms that can identify real-time abnormal gait patterns and adjust to different contexts automatically.

The implemented algorithm takes a time series approach whereby the incoming data is compared against a reference model that has been trained using the good or normal steps from the collected data. The algorithm runs the gyroscope data (angular velocity) and outputs an anomaly score which indicates how different is the data point in relation to the reference model. The algorithm defines threshold values that range from 0 to 1 to determine whether the incoming data is anomalous. Figure 18 shows the ataxic gait plot with a threshold value of 0.6, the algorithm correctly identifies the abnormal gait but also contains 1 false positive (FP) detection.

To evaluate the performance of the anomaly detection algorithm the following metrics have been considered:

- True positives (TP): Correspond to the number of steps or gait behavior patterns that are abnormal and were correctly classified as such.
- True negatives (TN): These are the number of instances where normal steps are

correctly classified as normal.

- False positives (FP): Refer to the number of instances where normal patterns were incorrectly classified as abnormal.
- False negatives (FN): Considers the number of abnormal steps that have been incorrectly classified as normal.
- Earliness:This metric explains the time taken to classify the readings as an abnormal gait pattern. The time starts at the beginning of a step until the abnormality has been detected. This metric differs for all the gait disorders and it does not influence on the speed of detection.

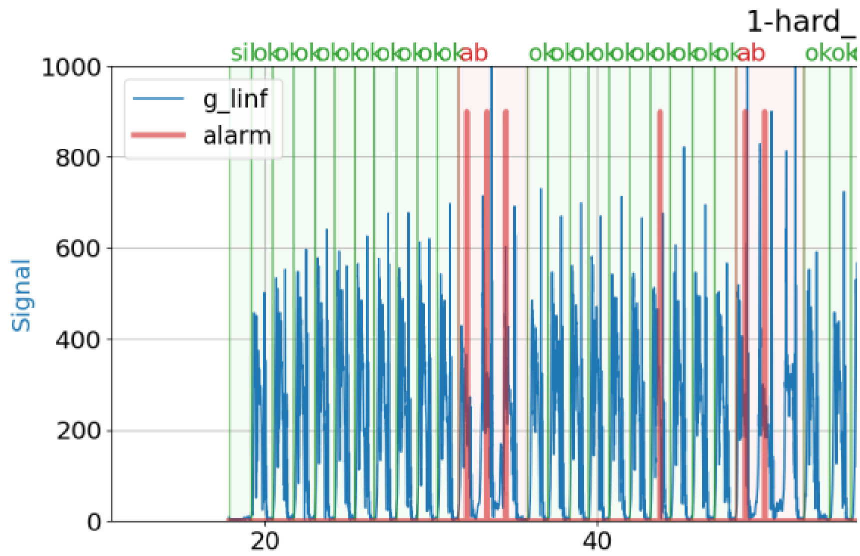

Figure 18. *Anomaly detection algorithm with a threshold of 0.6. The red lines represent the alarm which shows the earliness of detection.*

Subsequently, we consider examining the accuracy of the algorithm using the True Positive Rate (5.1) and the False Positive Rate (5.1). The True Positive Rate, also known as 'Recall' measures the proportion of abnormal patterns that are correctly identified as such. Similarly, FPR or 'Fall-Out', is the proportion of abnormal patterns incorrectly identified as normal cases.

True Positive Rate

$$TPR = \frac{TP}{TP + FN} \tag{5.1}$$

False Positive Rate

$$FPR = \frac{FP}{FP + TN} \tag{5.2}$$

Accuracy

$$ACC = \frac{TP + TN}{TP + FP + TN + FN} \tag{5.3}$$

Nevertheless, we cannot depend on the accuracy metric to evaluate the effectiveness of the algorithm, since it is a performance metric generally used when the data has an equal distribution or is balanced. So, we refer to other relevant metrics such as precision and recall which can be balanced and combined into a single metric i.e., the F1 score.

F1 score is defined as the harmonic mean of precision and recall, represented mathematically as:

$$F1 = \frac{2TP}{2TP + FP + FN} \tag{5.4}$$

It provides equal weight to both metrics, taking into consideration the data distribution hence its ample use when dealing with imbalanced data.

5.2 Experimental results using the prototype measuring system

Initially, the sensors were programmed to acquire readings at a sampling rate of $f_s = 100Hz$, ($t_s = 0.01s$), which resulted in large data loss and inconsistent transferring of the data via Bluetooth, so a new sampling rate was adopted ($f_s = 50Hz$)) with an associated period of $t_s = 0.02s$. Nevertheless, the outcomes of the assembled ESP32 measuring system prototype did not perform as expected.

Therefore, we decided to employ the spline resampling technique to refine the frequency resolution and test whether the problem was due to compatibility issues with the algorithm's data files format. The process of increasing the rate of the frequency by an L factor is called upsampling and in our case, the L value will be determined by the desired frequency. The current sampling rate is $f_s = 50Hz$ and now we upsample by a factor of 5.12, that is, $L = 5.12$. Hence, the sampling rate is increased to be $5.12 \times 50Hz = 256Hz$.

Overall, through resampling and interpolation we obtained signals that resembled the ones obtained using the Shimmer3 sensors, as can be see in Figure 20. However, unfortunately further analysis and processing of the acquired data is still needed, since the modified data sets still presented errors and could not provide any positive outcomes. As mentioned in section 3.1, the preferred alternative might be to switch microcontroller platforms or implement a compiled programming language. For that reason we will be analysing the results obtained through the implementation of the adaptive threshold shapelet-based algorithm musing the data acquired via the Shimmer 3 sensors.

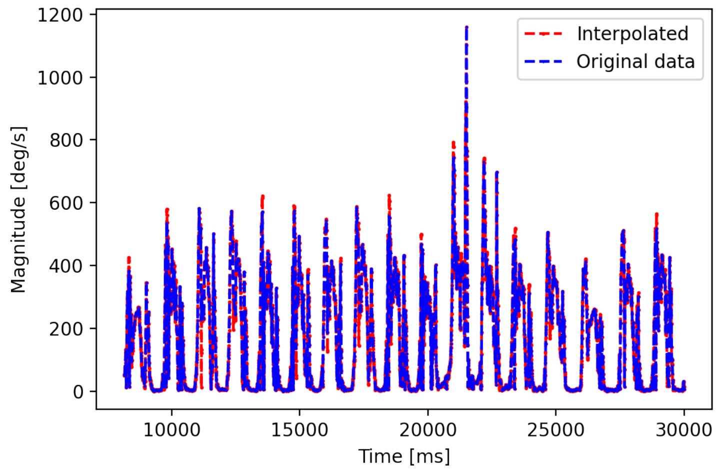

Figure 19. *Red:The gyroscope magnitude after upsampling and applying interpolation; Blue: The original data*

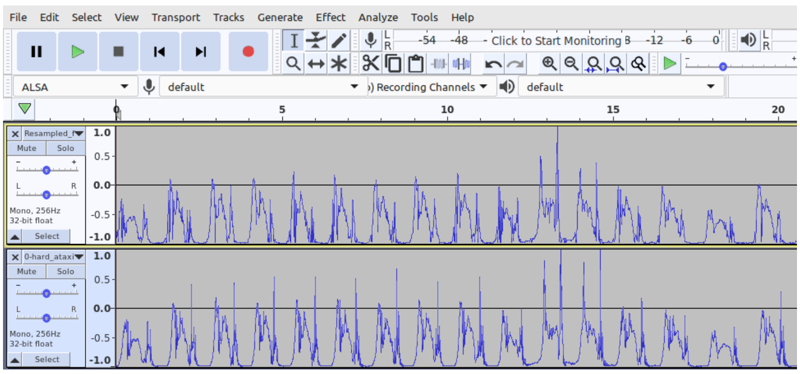

Figure 20. *Top:Resampled data (ataxic gait); Bottom: Shimmer3 data (ataxic gait)*

5.3 Experimental results using the Shimmer3 sensors

The overall accuracy and F1 scores achieved using the adaptive threshold shapelet-based algorithm are presented in tables 5 - 9. Different groups of data sets were selected to check whether the algorithm performed better when trained with various individual data sets or if it worked best with one person's data files. We report the mean and the standard deviation scores for each metric and divided the data into groups of different file sizes. Group 1 consists of two data files from one male participant, who performed each gait disorder simulation twice. Regrettably, the hemiplegic and diplegic data sets were removed due to the misclassification errors of the abnormal steps with an F1 score of 0%, most likely because the files were too short. Group 2 included 8 data files from four different participants who had similar height and weight but different ages (height [mean±std] 180.9 cm ± 2.45 , weight [mean±std] 81.29 Kg ± 7.87, and age [mean± std] 33.94 years± 16.64). Finally, Group 3 contained multiple data files from six different participants of varying gender, height, weight, and age.

We observe that Groups 2 and 3 have the same number of data files for antalgic and hemiplegic gait, since some data files had to be discarded due to errors with the data collection phase or the processing of the data. The occurrence of the errors may be partially explained the data sets had few readings and/or the behavior of the normal steps was difficult to characterize due to their dissimilarity.

The adaptive threshold-based algorithm outputs the base master metrics (TP, TN, FP, FN) from which Precision, Recall, Accuracy and F1 score were calculated from the mean values of the best threshold scores per anomaly. The algorithm shows good scores for parkinsonian gait detection: Accuracy and F1 scores are above 80% across all three groups.On the other hand, accuracy and F1 scores are the lowest for the antalgic gait anomaly detection, with the lowest F1 score being 46%. The poor performance of the algorithm could be attributed to the anomalous steps having a similar behavior as the normal steps. Accuracy, on the contrary has values above 86%. A probable reason is that the F1 score is based on Precision and Recall which do not account for TN values. As a result the high accuracy scores for antalgic gait compared to their F1 scores highlight that the percentage of TN values are higher than the others.

In Figure 21, we plot the F1 score results. Group 1 is the most effective, followed by Group 3. Whereas. Group 2's scores are lower than the other ones, but have a higher standard deviation, which is interesting to see since the data was selected based on similar anthropometric elements (height and weight), thus we can infer that the gait behavior is not significantly affected by the persons' height and weight but other factors such as age play an important roles, perhaps if we tested with data from a similar age group we could see less scattered values. Furthermore,other parameters like speed and stride length were not controlled since the participants were asked to walk freely and perform the simulation as naturally as possible.

Table 5. *Antalgic Gait (mean ± std)*

Combination	Precision	Recall	ACC	F1	Earliness
Group 1 (2 files)	66.7±0.00	83.3±0.24	93.4±0.02	**73.3±0.09**	1.21
Group 2 (8 files)	63.6±0.25	52.5±0.23	86.6±0.09	52.7±0.20	1.10
Group 3 (8 files)	51.10± 0.24	47.50± 0.32	87.40± 0.05	46.19± 0.26	1.12

Table 6. *Ataxic Gait (mean ± std)*

Combination	Precision	Recall	ACC	F1	Earliness
Group 1 (2 files)	92.9 ±0.10	100±0.00	96.0±0.01	73.3±0.05	0.84
Group 2 (8 files)	76.6±0.16	84.8±0.30	90.0±0.11	**77.16±0.23**	1.31
Group 3 (13 files)	75.31± 0.21	84.22±0.29	91.76± 0.09	76.0±4 0.23	0.93

Table 7. *Diplegic Gait (mean ± std)*

Combination	Precision	Recall	ACC	F1	Earliness
Group 1 (2 files)	NA	NA	NA	NA	NA
Group 2 (6 files)	69.0± 0.43	100.00± 0.00	71.0± 0.44	73.2± 0.39	0.59
Group 3 (7 files)	73.81± 0.40	100.00± 0.00	78.84± 0.36	**77.98± 0.35**	0.70

Table 8. *Parkinsonian Gait (mean ± std)*

Combination	Precision	Recall	ACC	F1	Earliness
Group 1 (2 files)	75.0 0.00	100.0± 0.00	96.0± 0.00	**85.7± 0.00**	0.84
Group 2 (6 files)	83.3 0.41	69.4± 0.48	96.0± 0.06	**85.7± 0.32**	1.31
Group 3 (10 files)	76.00± 0.28	98.33± 0.05	91.77± 0.13	82.59± 0.22	0.85

Table 9. *Steppage Gait (mean ± std)*

Combination	Precision	Recall	ACC	F1	Earliness
Group 1 (2 files)	87.5± 0.18	91.7± 0.12	97.1± 0.01	**88.3± 0.04**	0.60
Group 2 (6 files)	58.9± 0.39	59.7± 0.39	84.8± 0.16	55.3± 0.35	0.59
Group 3 (10 files)	54.83± 0.32	65.83± 0.42	90.20± 0.07	56.57± 0.34	0.61

Table 10. *Hemiplegic Gait (mean ± std)*

Combination	Precision	Recall	ACC	F1	Earliness
Group 1 (2 files)	NA	NA	NA	NA	NA
Group 2 (6 files)	54.7 ±0.43	79.2±0.40	68.7± 0.41	70.6± 0.30	0.68
Group 3 (4 files)	72.53 ± 0.22	100.00 ± 0.00	94.73 ± 0.05	**82.73 ± 0.14**	0.70

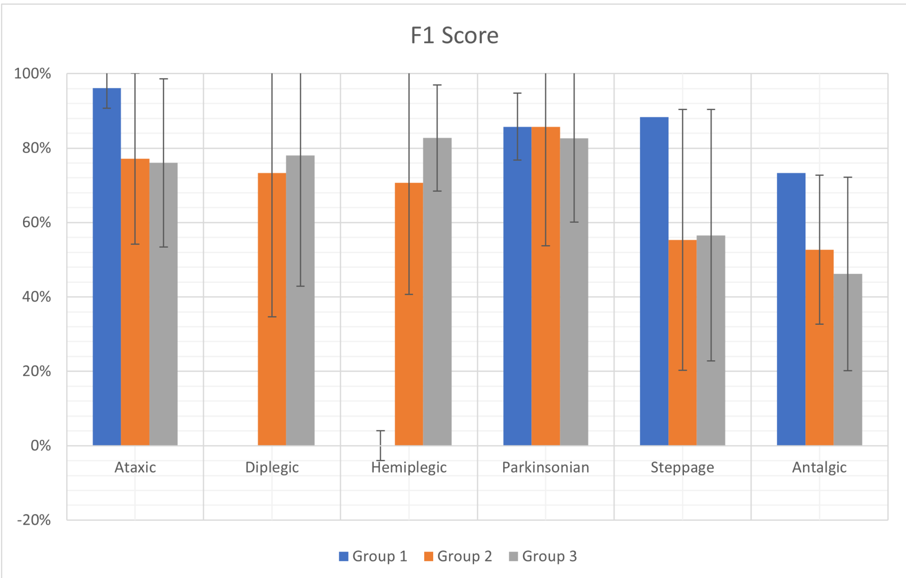

Figure 21. *F1 score results on all data sets grouped by the gait disorders considered in this thesis, while error bars depict the standard deviation.*

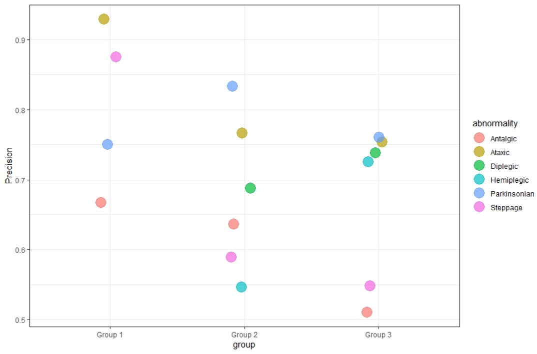

(a)

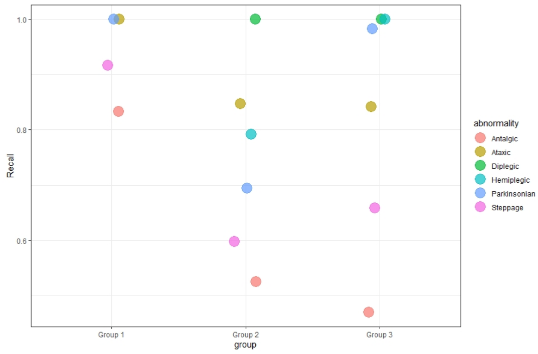

(b)

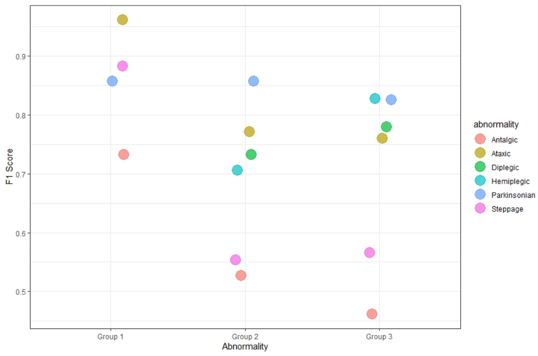

(c)

Figure 22. *Scatter plot of the test results. Each dot represents a different pathology. Results are grouped by combination. (a) Precision, (b) Recall, and (c) F1-score*

Furthermore, Figure 22 shows that Group 1 overall performs better on all three different performance metrics. It achieves the highest Recall and Precision score for Ataxic gait (100% and 93%, respectively), hence we can determine that this combination has a great capacity to detect gait abnormalities and high accuracy when detecting gait deviations. Overall, Group 1 is the most balanced combination and training the algorithm with the data from one person would be better since the normal step patterns differ from person to person and building a reference model of good steps with multitude of varying data might not provide the best outcomes.

Another interesting observation is represented in Table 11, where we compare the performance of the data from the sensors positioned below the knee (on top of the tibia) and the footbridge sensor.The highest values of the F1 score are highlighted in bold. Overall, the knee kinematics did not improve the algorithm's performance significantly except for the cases of hemiplegia and diplegia.We can see that the base metrics improve in the hemiplegic and diplegic gait disorders. This maybe due to the incremental influence of variations to the knee and hip movement characteristics of the hemiplegic gait as well as the scissor gait pattern (knees are flexed inwards with a narrow base) present in diplegic gait [47].

The weakness of the foot dorsiflexors appeared to play a major role to identify steppage gait, since the participants might have not correctly performed the knee flexion involved in steppage gait the data collected from the knee sensor performed poorly. On the other hand, the bending of the knee joint and the slow small steps present in the parkinsonian gait disorder, assisted in its correct classification having an F1 score of 90%. In the future more experiments involving patients with gait disorders will help determining the most suitable locations to place the sensors based on their needs and how the ailment progresses.

Table 11. *Mean and standard deviation for Precision, Recall, Accuracy and F1 score from five simulations.*

Pathology	Position	Precision	Recall	ACC	F1
Antalgia	BK	61.75%±0.20	93.06%± 0.06	91.90% ±0.05	72.75%±0.13
	FB	67.22%±0.13	94.44%± 0.10	93.49%± 0.04	**77.69%±0.10**
Ataxia	BK	72.92%±0.24	94.44%± 0.10	95.64%± 0.04	81.14% 0.16
	FB	75.95%±0.16	100.00%± 0.00	96.58% ±0.02	**85.62%±0.11**
Diplegia	BK	86.11%±0.24	100.00%± 0.00	97.78%±0.04	**91.23% 0.15**
	FB	73.33%±0.46	83.33%± 0.29	87.18%± 0.22	76.19%± 0.41
Hemiplegia	BK	62.89%±0.18	91.67%±0.08	91.58% ±0.04	**72.59%±0.09**
	FB	26.41% ±0.33	52.78%±0.21	56.82% ±0.34	33.77% ±0.29
Parkinson	BK	77.94% 0.15	100.00%± 0.00	95.97%± 0.04	86.98%± 0.10
	FB	83.33%± 0.14	100.00%± 0.00	97.52%± 0.02	**90.48%±0.08**
Steppage	BK	827.19%± 0.15	97.22%± 0.05	67.93%± 0.16	40.60%± 0.16
	FB	66.21%± 0.37	93.06%± 0.06	83.53%± 0.24	**71.30%±0.29**

5.4 Summary

In summary we have presented the results obtained after implementing the adaptive shapelet-based threshold algorithm using the data collected with the Shimmer3 sensors. Sadly, the designed prototype was not able to work at the desired sample rate and the collected data at a sampling rate of 50 Hz could not be used to run the program. So, we tried upsampling the data to 256 Hz but still could not run the algorithm due to errors with the Timestamp formatting presumably. Nevertheless, the current work has provided the researchers involved in project PRG424 an insight on the applicability of the present configuration, leading the team to opt for different microcontroller platforms. The results showed in this section indicated that the algorithm performs best when training with the data of a single individual as well as considering giving more importance to the type of gait disorder evaluated since the position of the sensor will have an impact on the algorithm's ability to detect the abnormalities, as was seen in the hemiplegic and setppage gait disorders.

6. Conclusions

The presented thesis describes the development and validation of a system to measure human gait motion from 20 abled-bodied individuals who simulated six different types o gait disorders. The components of the system were two BNO055 sensors and an ESP32 microcontroller deployed using MicroPython. The assessment of the device was going to be conducted by collecting data both with the prototype systems as well as with the Shimmer3 sensors so that we could validate its performance under the same conditions. Nevertheless, further work on developing the prototype is required so that the sensors can transmit the data in real-time with a sampling frequency above 100Hz.

The data collected using the Shimmer3 sensors was analyzed and used to test different configurations so that we could determine the future application of the device whether it was possible to obtain accurate results if the system had multiple people's data, would it be more capable of differentiating abnormal gait patterns? The analyzed results indicated that it was better to train and run the algorithm using the data from one individual at a time. Similarly, we concluded that sensor placement has a greater influence on the algorithm's ability to classify abnormal gait patterns, especially in disorders that involve hip and knee flexion. Future stages of the PRG424 project involve collecting data from actual patients which could help determine the sensor mapping on the body and also helping the researchers understand their needs and keep improving the design of the wearable FES electrode prototype.

All in all, the described system has proven through failure that the current setup is not viable and that switching to a different microcontroller platform or working around the inherent limitations of MicroPython in terms of storage management and speed could help imporve the perfromance of the device and ultimately provide people with gait impairments and physicians a device that adapts to the different recovery stages of the patient at an affordable cost.

References

[1] Tadeusz Mikolajczyk et al. “Advanced technology for gait rehabilitation: An overview”. In: *Advances in Mechanical Engineering* 10 (7 July 2018). ISSN: 16878140. DOI: 10.1177/1687814018783627.

[2] Catherine A Okoro et al. *Morbidity and Mortality Weekly Report Prevalence of Disabilities and Health Care Access by Disability Status and Type Among Adults-United States, 2016*. 2018. URL: https://aspe.hhs.gov/datacncl/standards/aca/4302/index.pdf..

[3] Adela Craciun. *CONVENȚIA PRIVIND DREPTURILE PERSOANELOR CU DIZABILITĂȚI*. Dec. 2013.

[4] Unated Nations. “World population ageing 2013”. In: *Department of Economic and Social Affairs PD* (2013).

[5] Lynne Turner-Stokes, Alan Bill, and Robert Dredge. “A cost analysis of specialist inpatient neurorehabilitation services in the UK”. In: *Clinical rehabilitation* 26.3 (2012), pp. 256–263.

[6] Luigi Tesio and Viviana Rota. “The Motion of Body Center of Mass During Walking: A Review Oriented to Clinical Applications”. In: *Frontiers in Neurology* 10 (Sept. 2019). ISSN: 16642295. DOI: 10.3389/fneur.2019.00999.

[7] A H M Ataullah, Orlando De Jesus drodejesus, and aolcom A H M Ataullah. *Gait Disturbances*. Nov. 2020. URL: https://www.statpearls.com/Keywords/Edit/22020.

[8] Hongliu Yu et al. *Assistive technology*. Vol. 1. World Intellectual Property Organization (WIPO), 2021, pp. 23–25. ISBN: 9789280532579.

[9] Walter Pirker and Regina Katzenschlager. *Gait disorders in adults and the elderly: A clinical guide*. Feb. 2017, pp. 81–95. DOI: 10.1007/s00508-016-1096-4.

[10] Gareth York and Samit Chakrabarty. “A survey on foot drop and functional electrical stimulation”. In: *International Journal of Intelligent Robotics and Applications* 3 (1 Mar. 2019), pp. 4–10. ISSN: 2366598X. DOI: 10.1007/s41315-019-00088-1.

[11] Diego Torricelli et al. “Human-like compliant locomotion: State of the art of robotic implementations”. In: *Bioinspiration and Biomimetics* 11 (5 Aug. 2016). ISSN: 17483190. DOI: 10.1088/1748-3190/11/5/051002.

[12] Fiona Coutts. “Gait analysis in the therapeutic environment”. In: *Manual Therapy* 4 (1 Feb. 1999), pp. 2–10. ISSN: 1356689X. DOI: 10.1016/S1356-689X(99)80003-4.

[13] Christopher L. Vaughan. “Theories of bipedal walking: An odyssey”. In: *Journal of Biomechanics* 36 (4 Apr. 2003), pp. 513–523. ISSN: 00219290. DOI: 10.1016/S0021-9290(02)00419-0.

[14] Sandra Shultz, David Perrin, and Peggy Houglum. *Examination of Musculoskeletal Injuries*. 4th Edition. Human Kinetics, 2016, pp. 55–63.

[15] Abdul Saboor et al. *Latest research trends in gait analysis using wearable sensors and machine learning: A systematic review*. 2020, pp. 167830–167864. DOI: 10.1109/ACCESS.2020.3022818.

[16] David Andreu et al. “Wireless Electrical Stimulators and Sensors Network for Closed Loop Control in Rehabilitation”. In: *Frontiers in Neuroscience* 14 (Feb. 2020). ISSN: 1662453X. DOI: 10.3389/fnins.2020.00117.

[17] Ethne L. Nussbaum et al. “Neuromuscular Electrical Stimulation for Treatment of Muscle Impairment: Critical Review and Recommendations for Clinical Practice”. In: *Physiotherapy Canada* 69 (5 Nov. 2017), pp. 1–76. ISSN: 0300-0508. DOI: 10.3138/ptc.2015-88.

[18] Naama Karniel et al. “Functional electrical stimulation compared with ankle-foot orthosis in subacute post stroke patients with foot drop: A pilot study”. In: *Assistive Technology* 33 (1 Jan. 2021), pp. 9–16. ISSN: 1040-0435. DOI: 10.1080/10400435.2019.1579269.

[19] Javier Gil-Castillo et al. “Advances in neuroprosthetic management of foot drop: A review”. In: *Journal of NeuroEngineering and Rehabilitation* 17 (1 Mar. 2020). ISSN: 17430003. DOI: 10.1186/s12984-020-00668-4.

[20] Shaun O’Connell and Alison Forrester. *Functional Electrical Stimulation Commissioning Statement*. NHS Vale of York, June 2018.

[21] Cep. *CEP10012 - Economic report: Functional electrical stimulation for drop foot of central neurological origin*. 2010.

[22] Edward Tobias. *Test-Walking the New Bioness L300 Go*. 2016. URL: https://multiplesclerosisnewstoday.com/2017/09/26/ms-test-walking-the-new-bioness-l300-go/.

[23] Shenzhen XFT Electronics. *Foot drop system*. 2022.

[24] G.M. Lyons et al. “A review of portable FES-based neural orthoses for the correction of drop foot”. In: *IEEE Transactions on Neural Systems and Rehabilitation Engineering* 10 (4 Dec. 2002), pp. 260–279. ISSN: 1534-4320. DOI: 10.1109/TNSRE.2002.806832.

[25] Lin Meng et al. “A functional electrical stimulation system for human walking inspired by reflexive control principles”. In: *Proceedings of the Institution of Mechanical Engineers, Part H: Journal of Engineering in Medicine* 231 (4 Apr. 2017), pp. 315–325. ISSN: 0954-4119. DOI: 10.1177/0954411917693879.

[26] Keitaro Shioiri et al. “Radar-based Gait Classification of Elderly Non-Fallers and Multiple Fallers Using Machine Learning”. In: IEEE, Mar. 2021, pp. 399–400. ISBN: 978-1-6654-1875-1. DOI: 10.1109/LifeTech52111.2021.9391835.

[27] Andrea Mannini and Angelo Maria Sabatini. “Gait phase detection and discrimination between walking–jogging activities using hidden Markov models applied to foot motion data from a gyroscope”. In: *Gait Posture* 36 (4 Sept. 2012), pp. 657–661. ISSN: 09666362. DOI: 10.1016/j.gaitpost.2012.06.017.

[28] Trung Thanh Ngo et al. “Similar gait action recognition using an inertial sensor”. In: *Pattern Recognition* 48 (4 Apr. 2015), pp. 1289–1301. ISSN: 00313203. DOI: 10.1016/j.patcog.2014.10.012.

[29] Mo Chen et al. “A self-adaptive foot-drop corrector using functional electrical stimulation (FES) modulated by tibialis anterior electromyography (EMG) dataset”. In: *Medical Engineering & Physics* 35 (2 Feb. 2013), pp. 195–204. ISSN: 13504533. DOI: 10.1016/j.medengphy.2012.04.016.

[30] N. Fränzel et al. “A prototyping system for smart wheelchairs”. In: *Biomedizinische Technik* 59 (Oct. 2014), S902–S905. ISSN: 00135585. DOI: 10.1515/bmt-2014-5011.

[31] Markus Valtin et al. “RehaMovePro: A versatile mobile stimulation system for transcutaneous FES applications”. In: *European Journal of Translational Myology* 26 (3 June 2016). ISSN: 2037-7460. DOI: 10.4081/ejtm.2016.6076.

[32] Djordje Slijepcevic et al. “Explaining Machine Learning Models for Clinical Gait Analysis”. In: *ACM Transactions on Computing for Healthcare* 3 (2 Apr. 2022). ISSN: 26378051. DOI: 10.1145/3474121.

[33] Ali Chelli and Matthias Patzold. “A Machine Learning Approach for Fall Detection and Daily Living Activity Recognition”. In: *IEEE Access* 7 (2019), pp. 38670–38687. ISSN: 21693536. DOI: 10.1109/ACCESS.2019.2906693.

[34] Abdul Hakim et al. “Smartphone Based Data Mining for Fall Detection: Analysis and Design”. In: vol. 105. Elsevier B.V., 2017, pp. 46–51. DOI: 10.1016/j.procs.2017.01.188.

[35] Praveen Kumar Pakkirisamy et al. *Optimal placement for IMU sensors on foot to extract gait parameters.* 2019. URL: http://ieeexplore.ieee.org/document/8324015/Viewproject.

[36] Kee S. Moon et al. "Identification of gait motion patterns using wearable inertial sensor network". In: *Sensors (Switzerland)* 19 (22 Nov. 2019). ISSN: 14248220. DOI: 10.3390/s19225024.

[37] Thomas Johann Seebeck. *LOW COST HIGH PRECISION DEVICE FOR 3D ORIENTATION*. 2016.

[38] Jermaine Smith and Yohannes Ketema. *Real-Time Position Tracking Using IMU Data*. URL: https://www.reichelt.com/de/en/arduino-uno-rev-3-atmega328-usb-arduino-uno-p119045.html.

[39] Peter Hinch. *MicroPython BNO055*. URL: https://github.com/micropython-IMU/micropython-bno055. (accessed: 07.27.2022).

[40] Damien P. George. *low-level Bluetooth*. URL: https://docs.micropython.org/en/latest/library/bluetooth.html. (accessed: 07.27.2022).

[41] George Bantique. "ESP32 MicroPython: ESP32 Bluetooth Low Energy". In: (Aug. 2021).

[42] Thomas Seel, Cordula Werner, and Thomas Schauer. "The adaptive drop foot stimulator – Multivariable learning control of foot pitch and roll motion in paretic gait". In: *Medical Engineering and Physics* 38 (11 Nov. 2016), pp. 1205–1213. ISSN: 18734030. DOI: 10.1016/j.medengphy.2016.06.009.

[43] Shimmer. *IMU User Guide Revision 1.4*. 2016.

[44] Ulvi Ahmod. *THE CONTEXT SENSITIVE GAIT MONITORING FOR PATIENT SUPPORT*. Tallinn University of Technology, May 2021.

[45] Nilesh Barla. *Data Annotation Tutorial: Definition, Tools, Datasets*. Mar. 2022.

[46] Zena M. Hira and Duncan F. Gillies. "A Review of Feature Selection and Feature Extraction Methods Applied on Microarray Data". In: *Advances in Bioinformatics* 2015 (June 2015), pp. 1–13. ISSN: 1687-8027. DOI: 10.1155/2015/198363.

[47] Christopher D. Stephen et al. "Phasic Knee Bending Dystonic and Parkinsonian Gait: A Characteristic Finding in <scp>X-Linked</scp> Dystonia Parkinsonism". In: *Movement Disorders Clinical Practice* 7 (4 May 2020), pp. 448–452. ISSN: 2330-1619. DOI: 10.1002/mdc3.12929.

Appendix 1 – Non-Exclusive License for Reproduction and Publication of a Graduation Thesis[1]

I Fiorella Ines Soto Sanchez

1. Grant Tallinn University of Technology free licence (non-exclusive licence) for my thesis “Contributing to the development of the next generation neuroprosthetic device: data collection, processing, and prototype development”, supervised by Alar Kussik and Jakob Rostovski
   1.1. to be reproduced for the purposes of preservation and electronic publication of the graduation thesis, incl. to be entered in the digital collection of the library of Tallinn University of Technology until expiry of the term of copyright;
   1.2. to be published via the web of Tallinn University of Technology, incl. to be entered in the digital collection of the library of Tallinn University of Technology until expiry of the term of copyright.
2. I am aware that the author also retains the rights specified in clause 1 of the non-exclusive licence.
3. I confirm that granting the non-exclusive licence does not infringe other persons’ intellectual property rights, the rights arising from the Personal Data Protection Act or rights arising from other legislation.

16.08.2022

[1] The non-exclusive licence is not valid during the validity of access restriction indicated in the student’s application for restriction on access to the graduation thesis that has been signed by the school’s dean, except in case of the university’s right to reproduce the thesis for preservation purposes only. If a graduation thesis is based on the joint creative activity of two or more persons and the co-author(s) has/have not granted, by the set deadline, the student defending his/her graduation thesis consent to reproduce and publish the graduation thesis in compliance with clauses 1.1 and 1.2 of the non-exclusive licence, the non-exclusive license shall not be valid for the period.